

**Charge ordering, ferroelectric, and magnetic domains in LuFe<sub>2</sub>O<sub>4</sub> observed by scanning probe microscopy**

I. K. Yang, Jeehoon Kim, S. H. Lee, S.-W. Cheong, and Y. H. Jeong

Citation: [Applied Physics Letters](#) **106**, 152902 (2015); doi: 10.1063/1.4918358

View online: <http://dx.doi.org/10.1063/1.4918358>

View Table of Contents: <http://scitation.aip.org/content/aip/journal/apl/106/15?ver=pdfcov>

Published by the [AIP Publishing](#)

---

**Articles you may be interested in**

[Resonant photoemission study of multiferroic LuFe<sub>2</sub>O<sub>4</sub> across three-dimensional to two-dimensional charge ordering](#)

Appl. Phys. Lett. **106**, 172905 (2015); 10.1063/1.4919726

[Oxygen stoichiometry and magnetic properties of LuFe<sub>2</sub>O<sub>4+δ</sub>](#)

J. Appl. Phys. **113**, 063909 (2013); 10.1063/1.4792036

[Spin-charge-orbital coupling in multiferroic LuFe<sub>2</sub>O<sub>4</sub> thin films](#)

Appl. Phys. Lett. **100**, 212904 (2012); 10.1063/1.4720401

[Ferroic investigations in LuFe<sub>2</sub>O<sub>4</sub> multiferroic ceramics](#)

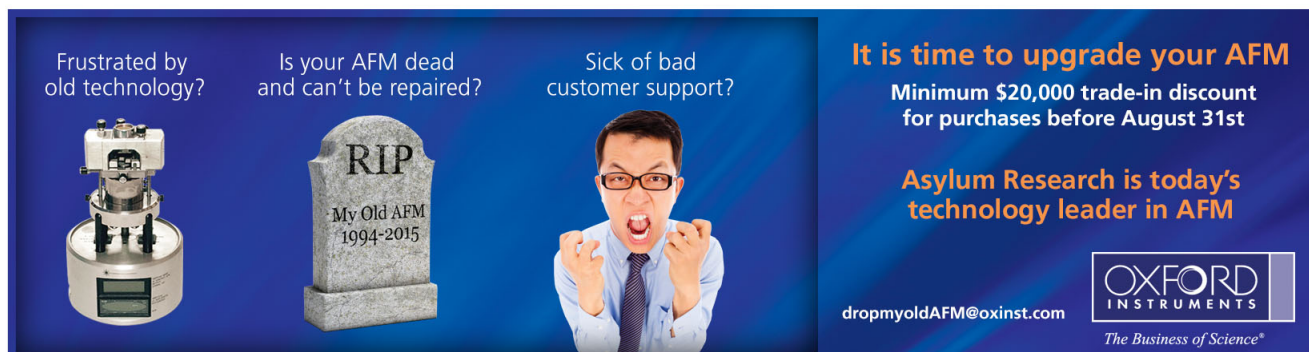
J. Appl. Phys. **110**, 034108 (2011); 10.1063/1.3622147

[Dynamic magnetoelectric coupling in “electronic ferroelectric” Lu Fe 2 O 4](#)

Appl. Phys. Lett. **91**, 152903 (2007); 10.1063/1.2798597

---

Frustrated by old technology?      Is your AFM dead and can't be repaired?      Sick of bad customer support?



**It is time to upgrade your AFM**  
Minimum \$20,000 trade-in discount for purchases before August 31st

**Asylum Research is today's technology leader in AFM**

[dropmyoldAFM@oxinst.com](mailto:dropmyoldAFM@oxinst.com)

**OXFORD INSTRUMENTS**  
The Business of Science®

# Charge ordering, ferroelectric, and magnetic domains in LuFe<sub>2</sub>O<sub>4</sub> observed by scanning probe microscopy

I. K. Yang,<sup>1</sup> Jeehoon Kim,<sup>1,2</sup> S. H. Lee,<sup>3</sup> S.-W. Cheong,<sup>4,5</sup> and Y. H. Jeong<sup>1,a)</sup>

<sup>1</sup>Department of Physics, POSTECH, 77 Cheongam-Ro, Pohang 790-784, South Korea

<sup>2</sup>CALDES, Institute of Basic Science, 77 Cheongam-Ro, Pohang 790-784, South Korea

<sup>3</sup>YE Team, Samsung Electronics, 1 Samsungjeonja-Ro, Hwaseong 445-330, South Korea

<sup>4</sup>Laboratory of Pohang Emergent Materials, POSTECH, 77 Cheongam-Ro, Pohang 790-784, South Korea

<sup>5</sup>Department of Physics and Astronomy, Rutgers University, Piscataway, New Jersey 08854, USA

(Received 11 November 2014; accepted 6 April 2015; published online 14 April 2015)

LuFe<sub>2</sub>O<sub>4</sub> is a multiferroic system which exhibits charge order, ferroelectricity, and ferrimagnetism simultaneously below  $\sim 230$  K. The ferroelectric/charge order domains of LuFe<sub>2</sub>O<sub>4</sub> are imaged with both piezoresponse force microscopy (PFM) and electrostatic force microscopy (EFM), while the magnetic domains are characterized by magnetic force microscopy (MFM). Comparison of PFM and EFM results suggests that the proposed ferroelectricity in LuFe<sub>2</sub>O<sub>4</sub> is not of usual displacive type but of electronic origin. Simultaneous characterization of ferroelectric/charge order and magnetic domains by EFM and MFM, respectively, on the same surface of LuFe<sub>2</sub>O<sub>4</sub> reveals that both domains have irregular patterns of similar shape, but the length scales are quite different. The domain size is approximately 100 nm for the ferroelectric domains, while the magnetic domain size is much larger and gets as large as 1  $\mu$ m. We also demonstrate that the origin of the formation of irregular domains in LuFe<sub>2</sub>O<sub>4</sub> is not extrinsic but intrinsic. © 2015 AIP Publishing LLC.

[<http://dx.doi.org/10.1063/1.4918358>]

LuFe<sub>2</sub>O<sub>4</sub> is a multiferroic compound which exhibits both ferroelectricity ( $T_{FE} \approx 340$  K) and ferrimagnetism ( $T_N \approx 230$  K) in a single phase at low temperatures.<sup>1</sup> This material has attracted much attention particularly because of its peculiar origin of ferroelectricity. Ferroelectric materials may be classified into proper and improper ferroelectrics depending on whether ferroelectricity itself is a primary order parameter or not. Many recently discovered multiferroics are improper ferroelectrics, and magnetic ordering is responsible for the ferroelectricity.<sup>2,3</sup> The proposed ferroelectricity of LuFe<sub>2</sub>O<sub>4</sub> also appears to be improper; it is claimed to be of electronic origin and caused by charge ordering (CO).<sup>4</sup> This class would be termed *electronic* ferroelectricity. One possible consequence of electronic ferroelectricity due to electronic charge redistribution in the unit cell would be small or lack of piezoelectricity as opposed to normal displacive ferroelectrics where piezoelectricity necessarily appears.<sup>5</sup> It should be pointed out, however, that there are conflicting reports showing that this material may not be ferroelectric.<sup>6,7</sup> These authors have measured P-E hysteresis loops and dielectric properties, and concluded that LuFe<sub>2</sub>O<sub>4</sub> has a three dimensional CO phase but does not show spontaneous polarization. Thus, the genuineness of the ferroelectricity of LuFe<sub>2</sub>O<sub>4</sub> is still in dispute, and further investigations are needed to settle the issue. As is generally known, it is difficult to observe P-E hysteresis loops for materials with nonzero conductivity such as LuFe<sub>2</sub>O<sub>4</sub>. For our LuFe<sub>2</sub>O<sub>4</sub> single crystals, it was also difficult to prove or disprove the ferroelectricity of the ordered phase by direct polarization measurements. We temporarily assume that LuFe<sub>2</sub>O<sub>4</sub> is ferroelectric in the presence of definite proof

which sparked intense interest,<sup>1,4</sup> but our data and associated discussions would still hold even if proven otherwise.

Previous studies on LuFe<sub>2</sub>O<sub>4</sub> have revealed many interesting phenomena such as sequential CO transitions (two dimensional CO at 530 K and three dimensional CO at 340 K),<sup>8,9</sup> a huge coercive magnetic field reaching 10 T at 4 K,<sup>10</sup> a large magnetoelectric coupling at room temperature,<sup>11</sup> and electric field driven phase transitions.<sup>12,13</sup> It should be noted, however, that most of these studies were concerned with bulk properties as probed by macroscopic measurements, reciprocal mapping by X-ray scattering, neutron scattering, and electron diffraction. In order to further understand the complex physics of LuFe<sub>2</sub>O<sub>4</sub>, real space measurements of multiferroic properties would be helpful and, in particular, detailed investigations of the domain structures of LuFe<sub>2</sub>O<sub>4</sub> would provide new insights for the system. Previously, magnetic domains imaged into the *ab*-plane by magnetic force microscopy (MFM)<sup>10,14</sup> and CO domains viewed from the cross-section plane (containing the *c*-axis) imaged by Transmission Electron Microscopy (TEM)<sup>14–16</sup> were reported. If the origin of the ferroelectricity in LuFe<sub>2</sub>O<sub>4</sub> is indeed CO, the CO domains imaged by TEM can be considered as ferroelectric domains. The three dimensional (3D) structure of the magnetic domains of LuFe<sub>2</sub>O<sub>4</sub> has been proposed based on the *ab*-plane MFM images and the correlation length along the *c*-axis extracted from neutron scattering. The structure of the ferroelectric domains, on the other hand, can only be conjectured due to the lack of the corresponding domain structure information viewed from the *c*-direction (*ab*-plane imaging). Once the ferroelectric domain structure in the *ab*-plane is observed, it is possible to properly estimate the 3D ferroelectric domain structure by combining the information with the cross-section CO domain images by TEM. It is also important to compare the

<sup>a)</sup>Author to whom correspondence should be addressed. Electronic mail: yhj@postech.ac.kr

ferroelectric domain structure with the *ab*-plane magnetic domain structure to understand the possible correlations between the ferroelectric and magnetic orders in  $\text{LuFe}_2\text{O}_4$ .

In this letter, we report ferroelectric/CO as well as magnetic domain images on the *ab*-plane of  $\text{LuFe}_2\text{O}_4$  by various scanning probe microscopy (SPM) methods such as electrostatic force microscopy (EFM),<sup>17</sup> piezoresponse force microscopy (PFM),<sup>18</sup> and MFM.<sup>19</sup>  $\text{LuFe}_2\text{O}_4$  single crystals were grown by a floating zone crystal growing facility (SC1-MDH11020) from Canon Machinery. The typical size of single crystals was  $1\text{ mm} \times 1\text{ mm} \times 0.1\text{ mm}$ . EFM, PFM, and MFM measurements were carried out using two scanning probe microscopes (XE-100, PSIA and UHV-VT SPM, Omicron) equipped with corresponding tips. PFM and EFM images are compared to check the origin of the ferroelectricity. We also present various real space domain images measured by EFM and MFM and critically compare ferroelectric and magnetic domain structures, both of which turned out to be of irregular shape. We discuss these results with respect to the origin of the irregular domain formation.

The crystal structure of  $\text{LuFe}_2\text{O}_4$  consists of two types of oxide layers; one type is a lutetium oxide layer, and the other one is an iron oxide bilayer. With alternate stacking of these two types of layers, the unit cell of  $\text{LuFe}_2\text{O}_4$  is formed as shown in Fig. 1(a). The iron oxide bilayer plays a predominant role in determining both magnetic and ferroelectric properties of the system. If one focuses on the Fe ions, the bilayer is a double layer of stacked Fe triangular lattices. It is believed that in the ferroelectric phase, Fe ions assume two distinct oxidation states,  $\text{Fe}^{2+}$  and  $\text{Fe}^{3+}$ , and the double layer is divided into  $\text{Fe}^{2+}$ -rich and  $\text{Fe}^{3+}$ -rich layers. The  $\text{Fe}^{2+}$  ions in the  $\text{Fe}^{2+}$ -rich layer form a honeycomb arrangement with  $\text{Fe}^{3+}$  located at the center of each hexagon, and vice versa. This particular CO of  $\text{Fe}^{2+}$  and  $\text{Fe}^{3+}$  ions then leads to a charge imbalance between the layers within a bilayer and thus produces corresponding electric dipoles and ultimately ferroelectricity in the system.<sup>1,4</sup> Fe ions also carry unpaired spins corresponding to the oxidation states, and the exchange interactions between Fe ions yield ferrimagnetism with

geometrical frustration due to the triangular nature of the lattice.<sup>20,21</sup> Fig. 1(b) shows the magnetization of  $\text{LuFe}_2\text{O}_4$  as a function of temperature. Magnetic properties and resistivity were measured with a Physical Properties Measurement System (PPMS) from Quantum Design. The ferrimagnetic Curie temperature is  $\sim 230\text{ K}$ , which agrees with the previous reports.<sup>22,23</sup> The difference between the out-of-plane and the in-plane moments implies that the magnetic easy axis of this material is parallel to the *c*-axis. This result is in line with the previously proposed model of Ising-type ferrimagnetic order along the *c*-axis.<sup>10</sup> Considering that the magnetization of  $\text{LuFe}_2\text{O}_4$  lies along the *c*-axis, MFM measurements would be performed in the *ab*-plane of the sample. Fig. 1(c) is the semi-logarithmic plot of resistivity  $\rho$  in the *ab*-plane as a function of temperature; the resistivity exhibits an insulating behaviour ( $d\rho/dT < 0$ ) in the whole temperature range. Note that a slope change in  $\log \rho$  occurs rather gradually around  $340\text{ K}$  as highlighted in the inset. An increase in the absolute value of the slope  $|d \log \rho / dT|$  in the low temperature phase would be due to the three dimensional CO leading to the proposed ferroelectricity.<sup>6,24</sup>

Typical ferroelectric domains can be imaged by either EFM or PFM. EFM yields ferroelectric domain structures by detecting the surface electric potential which reflects surface polarization charges. PFM, on the other hand, detects the piezoresponse of ferroelectric domains, a length change in response to an applied voltage occurring in ferroelectric materials. As noted above, one may expect far smaller piezoelectricity from electronic ferroelectrics compared to displacive ones. Thus, we attempted to image the ferroelectric domains of  $\text{LuFe}_2\text{O}_4$  by both techniques and compare the results. It is known that the electric polarization of  $\text{LuFe}_2\text{O}_4$  is also parallel to the *c*-axis.<sup>1</sup> SPM tips are then to be brought to the *ab*-plane of  $\text{LuFe}_2\text{O}_4$  to probe the responses. It is technically critical to secure clean flat surfaces for SPM measurements; the layered structure of  $\text{LuFe}_2\text{O}_4$  allows cleaving and step-free flat *ab*-plane surfaces are easily obtained. (Note that the topographic images corresponding to EFM, PFM, or MFM results are shown in supplementary material.) Cleaved

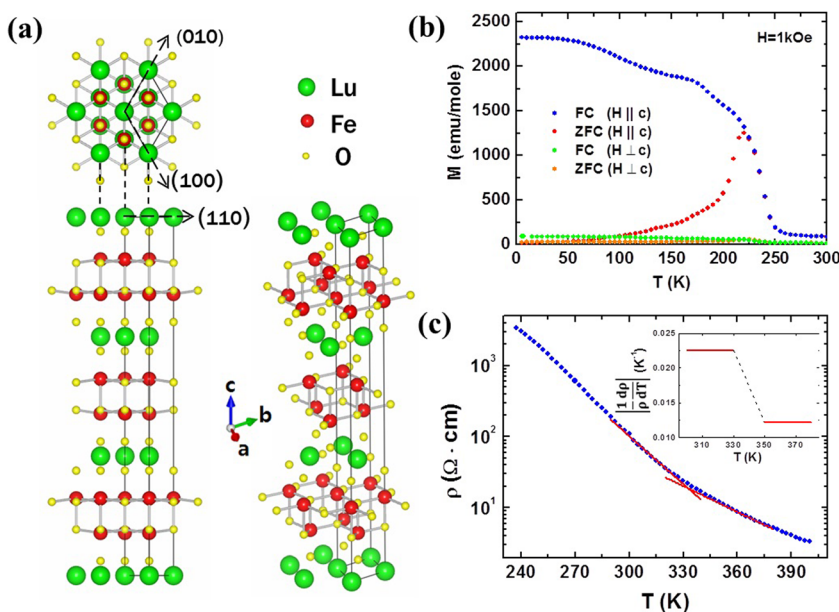


FIG. 1. (a) Crystal structure of  $\text{LuFe}_2\text{O}_4$ . (b) Temperature dependence of the magnetization parallel and perpendicular to the *c*-axis. Both field cooled (FC) and zero field cooled (ZFC) measurements with applied field  $1\text{ kOe}$  were performed. (c) Temperature dependence of in-plane resistivity. A slope change in  $\log \rho$ , as shown in the inset, occurs around  $340\text{ K}$  due to a ferroelectric charge ordering transition. The absolute slope was obtained from local fitting as indicated by solid lines.

LuFe<sub>2</sub>O<sub>4</sub> surfaces were first scanned by both EFM and PFM at room temperature. The ferroelectric domain structures were indeed observed by EFM and a typical image is shown in Fig. 2(a). The red and blue regions in the figure correspond to the surface charges due to up and down polarizations, respectively. The white regions are the domain boundaries or charge disordered regions. The ferroelectric domains have irregular patterns, and the average size of the domains is less than 100 nm. This unusual domain structure is discussed below in detail. For now, let us move on to the PFM results; Fig. 2(b) is the image of the same surface scanned by PFM measuring the vertical polarization component. It is remarkable that vertical PFM does not reveal any sign of a domain structure at all. Various efforts to improve the measurement sensitivity by changing frequency and amplitude of the AC probing voltage yielded the same image. This result obviously means that LuFe<sub>2</sub>O<sub>4</sub> lacks piezoelectricity; the absence of piezoelectricity in turn excludes a possibility of ferroelectricity of displacive type. Thus, the proposed ferroelectricity in LuFe<sub>2</sub>O<sub>4</sub> must be of unusual type such as the electronic one caused by CO. It is noted again that the ferroelectric domains in LuFe<sub>2</sub>O<sub>4</sub> we refer to in the present discussion are equivalent to CO domains.

The ferroelectric/charge order transition in LuFe<sub>2</sub>O<sub>4</sub> has previously been studied by various methods. The pyroelectric current measurement<sup>1</sup> and the temperature dependence of charge order superlattice spots<sup>9</sup> are representative examples in determining the phase transition temperature. In order to confirm the same transition by the SPM technique, EFM measurements were conducted as a function of temperature in heating direction from room temperature. Figs. 3(a) and 3(b) are the EFM images taken at 314 K and 390 K, respectively. In comparing the two images, the first thing to notice is a large difference in the contrast of the signal strength represented by the color images. This difference is attributed to the disappearing polarization as temperature increases above  $T_{FE}$ . According to the TEM study,<sup>9</sup> there still exists two dimensional CO even above  $T_{FE}$ . In order to obtain further information, EFM measurements at several temperatures are compared. Fig. 3(c) is a display of the average contrast as a function of temperature. The average contrast is obtained from a standard deviation in the signal strength histogram of each EFM image. It is seen that the contrast suddenly decreases between 330 K and 350 K. According to the resistivity data in Fig. 1(c), the ferroelectric CO transition temperature of LuFe<sub>2</sub>O<sub>4</sub> is located around 340 K. Thus, we may

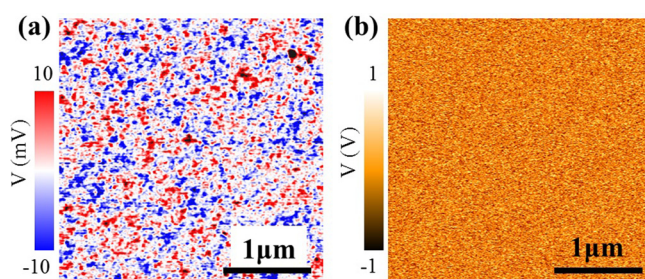


FIG. 2. (a) EFM image and (b) vertical PFM image of a cleaved *ab*-surface of LuFe<sub>2</sub>O<sub>4</sub> at room temperature. Red and blue colors in the EFM image indicate up and down domains of polarization, respectively.

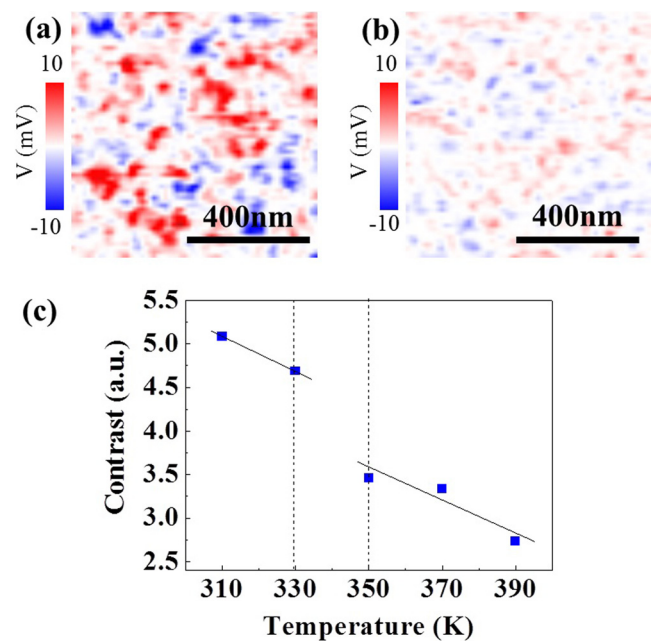


FIG. 3. EFM images obtained at (a) 314 K and (b) 390 K. The image size is  $\sim 800 \times 800 \text{ nm}^2$ . (c) Contrast, defined as a standard deviation in the signal strength histogram, is shown as a function of temperature. There is a break between 330 and 350 K. The solid lines are a guide to the eye.

conclude that the sudden drop in EFM image contrast is caused by the phase transition.

Now returning to the irregularity of the ferroelectric domains and its origin, it is noted that LuFe<sub>2</sub>O<sub>4</sub> is known to have several kinds of defects such as non-stoichiometric defects<sup>25</sup> and stacking faults.<sup>9</sup> Thus, it is important to check whether these defects are responsible for domain formation in any way. For this purpose, we have imaged by EFM exactly the same surface area at room temperature before and after annealing above the transition temperature. Figs. 4(a) and 4(b) are the domain images before and after annealing, respectively. It is easily seen from the figures that the general shape and qualitative features of the domain patterns remain unchanged but the exact locations of up and down domains have changed. If the domain formation is initiated by the defects in the sample and the domains are pinned by them, the locations of up and down domains in the two domain patterns should remain the same or at least similar because the annealing temperature is not high enough to change the defect positions. Thus, noting that the qualitative nature of the two domain patterns before and after annealing

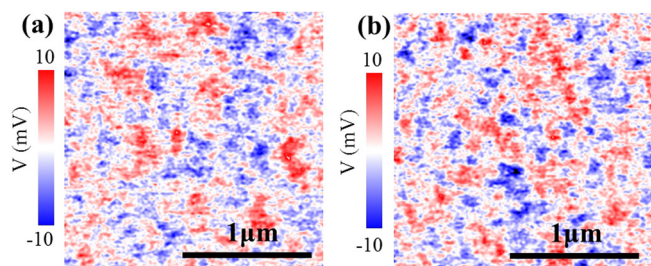


FIG. 4. EFM images at room temperature (a) before and (b) after annealing above the transition temperature of 340 K on a cleaved surface of LuFe<sub>2</sub>O<sub>4</sub>. The exact locations of up and down domains have changed, while the qualitative features of the domain patterns remain unchanged.

remains the same despite the fact that the exact locations of up and down domains are not reproducible, we conclude that the origin of the domain formation in  $\text{LuFe}_2\text{O}_4$  is intrinsic rather than extrinsic. The intrinsic property such as geometrical frustration inherent in the crystalline structure would be responsible for the irregular domain formation.

Having identified the general features of the ferroelectric domains, we wish to compare the ferroelectric and magnetic domains of  $\text{LuFe}_2\text{O}_4$ . In Figs. 5(a) and 5(b) displayed are the ferroelectric domains obtained by EFM and the magnetic domains by MFM, respectively. Figs. 5(a) and 5(b) were obtained by the same AFM at approximately 100 K, and the size of the images is the same as indicated by the scale bars in the figures. Note that the EFM signal strength represented in Fig. 5(a) is different from those of the previous EFM images because a different AFM and a different sample were used in the measurements. Nevertheless, the meaning of the colors remains unchanged. The MFM signals, represented in Fig. 5(b), were obtained as a frequency shift, and here again the red and blue colors denote the up and down magnetic domains, respectively. Although the domain structures in the ferroelectric and magnetic images are similar in shape, their average domain sizes are rather different. The similarity of the domains in shape would suggest the common cause. As mentioned in the introduction, both properties result from the ordering of  $\text{Fe}^{2+}$  and  $\text{Fe}^{3+}$  ions. For the magnetic domains, Wu *et al.*<sup>10</sup> proposed a model of pancake-like domains with disorder as the reason for the irregular magnetic domain pattern. We may also apply the pancake-like domain model to the ferroelectric domains. It should still be kept in mind, however, that the intrinsic geometrical frustration is indispensable for the irregular ferroelectric domains. The most distinctive difference between the ferroelectric and magnetic domains is their average size. The mean length of the irregular ferroelectric domains is estimated to be  $\sim 100$  nm; on the other hand, the size of the magnetic domains varies widely and the linear dimension even reaches  $\sim 1 \mu\text{m}$ . This large difference in length scale between the ferroelectric and magnetic domains is striking and visually conspicuous in Figs. 5(a) and 5(b).

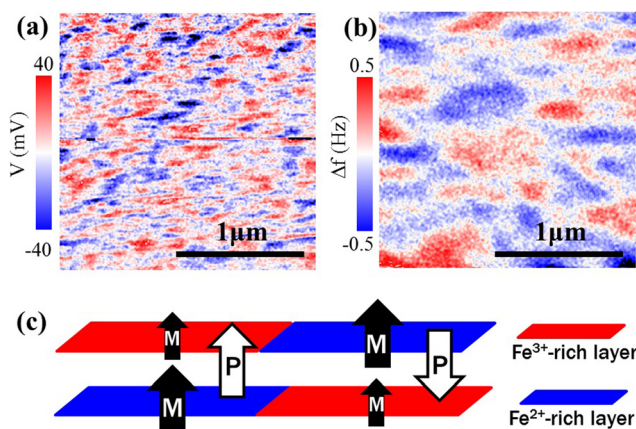


FIG. 5. (a) EFM and (b) MFM images of a  $\text{LuFe}_2\text{O}_4$  surface at 100 K. The large difference in length scale between the ferroelectric and magnetic domains is striking. Red and blue colors in the images indicate up and down domains of polarization or magnetization. (c) A schematic diagram of an iron oxide bilayer for a situation where a ferroelectric domain wall forms within a magnetic domain.

Recognizing the size difference in the ferroelectric and magnetic domains of  $\text{LuFe}_2\text{O}_4$ , we attempt to explain the domain size difference in the following way. As explained above, in  $\text{LuFe}_2\text{O}_4$ , the ferroelectric polarization is developed by separating an iron oxide bilayer into  $\text{Fe}^{2+}$ -rich and  $\text{Fe}^{3+}$ -rich layers, while the magnetization is determined by the direction of the magnetic moments of  $\text{Fe}^{2+}$  ( $S=2$ ) and  $\text{Fe}^{3+}$  ( $S=5/2$ ) which are not cancelled out in the ferrimagnetic configuration. Consider, as shown in Fig. 5(c), a bilayer which has two ferroelectric domains with opposite polarization. According to Ref. 21, the magnetic moments in the  $\text{Fe}^{2+}$ -rich and  $\text{Fe}^{3+}$ -rich layers point in the same direction as depicted in the figure. Note that the magnetic moment in the  $\text{Fe}^{2+}$ -rich layer is larger than that in the  $\text{Fe}^{3+}$ -rich layer. In this situation, EFM would be able to resolve the two domains, while MFM would not. MFM detects magnetic force arising between the tip and the sample, and the magnetic force on the tip resulting from the left and right domains in Fig. 5(c) is indistinguishable. Generally, an appearance of magnetic domain walls inside a ferroelectric domain would be excluded considering the high domain wall energy of  $\text{LuFe}_2\text{O}_4$  due to its exceptionally high magneto-crystalline anisotropy.<sup>10</sup>

In conclusion, we have imaged the ferroelectric/CO and magnetic domain structures within the *ab*-plane of  $\text{LuFe}_2\text{O}_4$  by SPM techniques which are non-destructive measurement tools. The simultaneous PFM and EFM measurements have suggested the non-displacive, electronic ferroelectricity in  $\text{LuFe}_2\text{O}_4$ . The EFM measurements as a function of temperature have identified a phase transition around 340 K, which agrees with the previous results measured by other means. The annealing investigations on the domain formation have shown that defects are not the main player for the domain location in  $\text{LuFe}_2\text{O}_4$ . Comparison of the ferroelectric and magnetic domain patterns has revealed a fact that the domain patterns share a similarity in shape but a difference in size exists. The former may be attributed to the geometrical frustration and charge disorder affecting the ordering of Fe ions which determines the electric and magnetic properties of  $\text{LuFe}_2\text{O}_4$ . The latter could result intrinsically from the different fluctuation behaviors of charge and magnetic degrees of freedom.

Y.H.J. wishes to thank S. Ishihara for useful discussions. This work was supported by the National Research Foundation (Grant No. 2011-0009231) and the Center for Topological Matter at POSTECH (Grant No. 2011-0030786). S.-W.C. was supported by the Max Planck POSTECH/KOREA Research Initiative Program (Grant No. 2011-0031558) through NRF. S.-W.C. was also supported by the NSF under Grant No. NSF-DMR-1104484.

<sup>1</sup>N. Ikeda, H. Ohsumi, K. Ohwada, K. Ishii, T. Inami, K. Kakurai, Y. Murakami, K. Yoshii, S. Mori, Y. Horibe, and H. Kito, *Nature(London)* **436**, 1136 (2005).

<sup>2</sup>W. Eerenstein, N. D. Mathur, and J. F. Scott, *Nature(London)* **442**, 759 (2006).

<sup>3</sup>S.-W. Cheong and M. Mostovoy, *Nat. Mater* **6**, 13 (2007).

<sup>4</sup>A. Nagano, M. Naka, J. Nasu, and S. Ishihara, *Phys. Rev. Lett.* **99**, 217202 (2007).

<sup>5</sup>See supplementary material at <http://dx.doi.org/10.1063/1.4918358> for argument accompanying this paper.

- <sup>6</sup>S. Lafuerza, J. Garcia, G. Subias, J. Blasco, K. Conder, and E. Pomjakushina, *Phys. Rev. B* **88**, 085130 (2013).
- <sup>7</sup>A. Ruff, S. Krohns, F. Schrettle, V. Tsurkan, P. Lunkenheimer, and A. Loidl, *Eur. Phys. J. B* **85**, 290 (2012).
- <sup>8</sup>Y. Yamada, K. Kitsuda, S. Nohdo, and N. Ikeda, *Phys. Rev. B* **62**, 12167 (2000).
- <sup>9</sup>Y. Zhang, H. X. Yang, Y. Q. Guo, C. Ma, H. F. Tian, J. L. Luo, and J. Q. Li, *Phys. Rev. B* **76**, 184105 (2007).
- <sup>10</sup>W. Wu, V. Kiryukhin, H.-J. Noh, K.-T. Ko, J.-H. Park, W. Ratcliff, P. A. Sharma, N. Harrison, Y. J. Choi, Y. Horibe, S. Lee, S. Park, H. T. Yi, C. L. Zhang, and S.-W. Cheong, *Phys. Rev. Lett.* **101**, 137203 (2008).
- <sup>11</sup>M. A. Subramanian, T. He, J. Chen, N. S. Rogado, T. G. Calvarese, and A. W. Sleight, *Adv. Mater.* **18**, 1737 (2006).
- <sup>12</sup>C. Li, X. Zhang, Z. Cheng, and Y. Sun, *Appl. Phys. Lett.* **93**, 152103 (2008).
- <sup>13</sup>L. J. Zeng, H. X. Yang, Y. Zhang, H. F. Tian, C. Ma, Y. B. Qin, Y. G. Zhang, and J. Q. Li, *Europhys. Lett.* **84**, 57011 (2008).
- <sup>14</sup>S. Park, Y. Horibe, Y. J. Choi, C. L. Zhang, S.-W. Cheong, and W. Wu, *Phys. Rev. B* **79**, 180401(R) (2009).
- <sup>15</sup>Y. Zhang, H. X. Yang, C. Ma, H. F. Tian, and J. Q. Li, *Phys. Rev. Lett.* **98**, 247602 (2007).
- <sup>16</sup>T. Maruyama, Y. Murakami, D. Shindo, N. Abe, and T. Arima, *Phys. Rev. B* **86**, 054202 (2012).
- <sup>17</sup>J. Ohgami, Y. Sugawara, S. Morita, E. Nakamura, and T. Ozaki, *Jpn. J. Appl. Phys., Part 1* **35**, 2734 (1996).
- <sup>18</sup>A. Gruverman, O. Auciello, and H. Tokumoto, *Annu. Rev. Mater. Sci.* **28**, 101 (1998).
- <sup>19</sup>D. Rugar, H. J. Mamin, P. Guethner, S. E. Lambert, J. E. Stern, I. McFadyen, and T. Yogi, *J. Appl. Phys.* **68**, 1169 (1990).
- <sup>20</sup>H. J. Xiang, E. J. Kan, S.-H. Wei, M.-H. Whangbo, and J. Yang, *Phys. Rev. B* **80**, 132408 (2009).
- <sup>21</sup>K.-T. Ko, H.-J. Noh, J.-Y. Kim, B.-G. Park, J.-H. Park, A. Tanaka, S. B. Kim, C. L. Zhang, and S.-W. Cheong, *Phys. Rev. Lett.* **103**, 207202 (2009).
- <sup>22</sup>J. Iida, M. Tanaka, Y. Nakagawa, S. Funahashi, N. Kimizuka, and S. Takekawa, *J. Phys. Soc. Jpn.* **62**, 1723 (1993).
- <sup>23</sup>F. Wang, J. Kim, and Y.-J. Kim, *Phys. Rev. B* **80**, 024419 (2009).
- <sup>24</sup>T. Kambe, Y. Fukada, J. Kano, T. Nagata, H. Okazaki, T. Yokoya, S. Wakimoto, K. Kakurai, and N. Ikeda, *Phys. Rev. Lett.* **110**, 117602 (2013).
- <sup>25</sup>H. X. Yang, H. F. Tian, Y. Zhang, Y. B. Qin, L. J. Zeng, C. Ma, H. L. Shi, and J. B. Lu, *Solid State Commun.* **150**, 1467 (2010).